

# Structural investigation of human dectin-1 receptor; A novel gateway in drug discovery

Talat Roome<sup>1</sup>, Yasmeen Rashid<sup>2\*</sup>, Muhammad Aurongzeb<sup>3</sup> and Anam Razzak<sup>1</sup>

<sup>1</sup>Molecular Pathology, Department of Pathology, Dow Diagnostic Reference and Research Laboratory, Dow International Medical College, Dow University of Health Sciences (Ojha Campus), Karachi, Pakistan

<sup>2</sup>Department of Biochemistry, University of Karachi, Karachi, Pakistan

<sup>3</sup>Jamil-ur-Rehman Center for Genome Research, International Center for Chemical and Biological Sciences, University of Karachi, Karachi, Pakistan

---

**Abstract:** Stimulation of C-type lectin domain of human dectin-1 receptor by fungal  $\beta$ -glucans causes conformational changes in its cytoplasmic domain which initiates various cellular responses mediated by downstream signaling components. We aimed to build the three-dimensional structures of the cytoplasmic domain as well as C-type lectin domain of human Dectin-1 along with their potential ligands through homology modeling. The overall three-dimensional fold of cytoplasmic domain was found to consist of mixed  $\beta$ -sheet whereas, in case of C-type lectin domain antiparallel  $\beta$ -sheets flanked by  $\alpha$ -helices were observed. Protein-protein docking strategy was utilized to monitor key interactions between cytoplasmic domain of dectin-1 receptor and PKC $\delta$ , as a prime regulator of Dectin-1 signaling. The interface was observed to have both hydrophilic and hydrophobic amino acid residues maintaining crucial contacts between the two proteins. The given three dimensional structural information can be implicated in structure-based drug designing to discover potential immunomodulators that can interfere with the immune responses and phagocytosis during inflammatory and infectious conditions.

**Keywords:** C-type lectin domain, cytoplasmic domain of Dectin-1 receptor, structural bioinformatics, homology modeling, molecular docking.

---

## INTRODUCTION

Dectin-1 is a Pattern Recognition Receptor (PRR) of innate immune system which is a type II transmembrane protein containing carbohydrate recognition domain (CRD) and immunoreceptor tyrosine-based activation motif (ITAM) at the extracellular C-terminal and intracellular N-terminal regions, respectively (Ariizumi, Shen *et al.* 2000, Adachi, Ishii *et al.* 2004). The CRD of Dectin-1 belongs to the C-type lectin-like domain (CTLD) subfamily and is considered as a non-classical C-type lectin because it lacks the calcium binding site in its C-terminal domain and its ITAM motif does not contain the distal tyrosine residue (Tyr-3) owing only proximal tyrosine residue (Tyr-15) within the single YXXL sequence (Underhill, Rossmagle *et al.* 2005, Underhill 2007). Dectin-1 was first identified on dendritic cells but was later found to be expressed on monocytes, macrophages, neutrophils and a subset of T cells (Brown and Gordon 2001, Taylor, Brown *et al.* 2002). This receptor is specific to bind with  $\beta$ -1,3- and  $\beta$ -1,6-linked glucans; pathogen associated molecular patterns (PAMPs); which are found to be present in fungal and microbial cell walls. Hence, the activation of Dectin-1 receptor causes phosphorylation of ITAM-Tyr-15 via Src kinase followed by docking of Syk kinase with the cytoplasmic domain of Dectin-1 receptor (CDDR). This

mechanism tends to stimulate different pro-inflammatory responses and host defense such as fungal uptake and production of cytokines and chemokines (Brown, Herre *et al.* 2003, Gantner, Simmons *et al.* 2003, Rogers, Slack *et al.* 2005). In our previous study, we have demonstrated that activation of Dectin-1 by zymosan (a copy of fungal pathogens) was found to be involved in the regulation of superoxide anion ( $O_2^-$ ) production via NADPH oxidase followed by phagocytosis. Additionally, protein kinase C- $\delta$  (PKC $\delta$ ) has been identified as a novel downstream signaling component of Dectin-1 receptor that directly bind with the Tyr-15 residue and form a molecular complex with Syk and Src kinases to drive the entire cellular immune response (Elsori, Yakubenko *et al.* 2011).

In chronic granulomatous disease, there is an inherited defect in NADPH oxidase activity that causes life threatening and recurrent infections due to severe depletion of  $O_2^-$ . Conversely, overproduction of  $O_2^-$  by activated monocytes results in oxidation of low density lipoproteins (LDLs) which leads to the formation of atherosclerotic plaque (Cathcart, McNally *et al.* 1989; Cathcart 2004). Moreover, superoxide anion radicals are the most potent stimuli responsible for increasing vascular permeability, enhancing pro-inflammatory cytokines and chemokines production as well as provoking DNA and tissue damage which augment the state of inflammation (Salvemini, Mazzon *et al.* 2001). Therefore, during fungal infections, it is important to limit the level of Dectin-1

---

\*Corresponding author: e-mail: yrashid2004@yahoo.com

mediated O<sub>2</sub><sup>-</sup> generation within the cell to ensure efficient host defense without causing chronic inflammation.

Considering all this, it is highly significant to determine the molecular structure of human Dectin-1 receptor and its interaction with the key signaling components to intervene the receptor functionality. Current post-genomic era focus on structural knowledge of protein complexes to understand how certain biomolecules work together in signal transduction pathways. Crystal structure of murine dectin-1 receptor complexed with fungal  $\beta$ -glucan has been determined (Brown, O'Callaghan *et al.* 2007). Recently, the three-dimensional (3D) homology model of Dectin-1 protein from *Bubalus bubalis* has been constructed and its molecular interaction with  $\beta$ -1,3 glucan has also been demonstrated (Yadav, Tripathi *et al.* 2012). The 3D structure of human Dectin-1 receptor has not been described so far. Considering the above mentioned role of CTLD and CDDR in ligand recognition and signaling of various cellular responses, respectively, it is important to determine their molecular structures and to understand their specific interaction patterns.

Homology modeling and molecular docking have been employed as cost-effective alternative methods for the 3D model construction and to predict accurate protein-protein and protein-ligand binding modes. Several 3D-structure modeling and molecular docking studies have been performed on specific proteins from pathogenic species for protein structure-function analysis (Azim 2011, Rashid and Kamran Azim 2011, Rashid, Kamran Azim *et al.* 2012). The present study was designed to perform homology modeling of CTLD and CDDR of Dectin-1 receptor for determination of their 3D folds and molecular characterization for exploring crucial interactions between CDDR and PKC $\delta$  (the prime regulator of Dectin-1 mediated immune responses). These findings can be implicated in biomedical research and rational drug designing to target various alarming and challenging inflammatory and immune diseases.

## MATERIALS AND METHODS

### *Sequence retrieval and secondary structure prediction*

During this study, amino acid sequences of human CDDR and CTLD were retrieved from Uniprot knowledgebase (Magrane and Consortium 2011) to carry out their sequence analyses. The secondary structure prediction was performed using PsiPred program (Jones 1999). The obtained secondary structural information was considered to improve the target-template sequence alignment.

### *Template search*

Due to poor sequence similarity of human CDDR protein within Protein Data Bank (Bernstein, Koetzle *et al.* 1977), structural homologue of human CDDR could not be identified traditionally by exercising Psi-BLAST search (Altschul, Madden *et al.* 1997). Therefore, the expected

three dimensional architecture of human CDDR protein was determined by pGen THREADER fold recognition method (Lobley, Sadowski *et al.* 2009) available at PsiPred Protein Structure Prediction Server (McGuffin, Bryson *et al.* 2000). All the parameters of pGen THREADER fold recognition method (Altschul, Madden *et al.* 1997) were used as default. On the other hand, the template of CTLD protein was identified using the Psi-BLAST tool (Ariizumi, Shen *et al.* 2000).

### *Homology modeling*

The three dimensional structures of templates i.e. *Pseudomonas sp.* L-aspartate  $\beta$ -decarboxylase (pdb id; 2ZY2) for CDDR homology modeling and murine Dectin-1 (pdb id; 2CL8) for CTLD homology modeling were retrieved from PDB (Bernstein, Koetzle *et al.* 1977) as text file. Both the template structures were analyzed for any missing residue and edited according to the final alignment. Secondary structure of *Pseudomonas sp.* L-aspartate  $\beta$ -decarboxylase (pdb id; 2ZY2) and predicted secondary structure of human CDDR protein were taken into considered for the generation of structure-based pair-wise sequence alignment so that maximum identity could be attained and gaps could be removed from regions of regular secondary structure. The finalized pair-wise sequence alignment was utilized as an input for homology model building by Modeller9.10 software (Sali 1995). Ten preliminary homology models including all non-hydrogen main chain and side chain atoms were generated.

### *Evaluation of homology models*

The ten preliminary homology models of both proteins were evaluated through different parameters. The potential energies of all the models were calculated through DOPE score command of the MODELLER 9.10(Sali 1995). The model with best DOPE score was further analyzed using Procheck (Laskowski, MacArthur *et al.* 1993) for the stereochemical compatibility. Energy profiles of the model and template were obtained by PROSA2003 software (Sippl 1993). The Prosa web server (Wiederstein and Sippl 2007) was employed to verify the local compatibility of the model related to genuine protein structures.

### *Protein three-dimensional structure visualization and modeling*

In order to display protein structures on the graphics screen in three dimensional mode, their structural investigations and manipulations including surface representations etc, 3D visualization and modeling programs were employed.

### *Molecular docking studies*

For CDDR and PKC $\delta$  protein-protein docking, HADDOCK software Web-portal (de Vries, van Dijk *et al.* 2010) was implemented. Regarding HADDOCK docking procedure, we used prediction interface which

utilizes CPORT interface predictor. CPORT is an algorithm which predicts amino acid residues implicated in protein-protein interface. By combining six interface prediction methods into a consensus predictor, CPORT provides potential surface residues predictions to HADDOCK (de Vries and Bonvin 2011). The docked solutions were analyzed and compared using DSVisualizer (<http://www.biocompare.com/review/470/Accelrys-DS-Viewer-50.html>) and Ligplus (Laskowski and Swindells 2011) softwares.

### Multiple sequence alignment

The human PKC $\delta$  protein sequence was searched against UniProtKb database (Magrane and Consortium 2011) using FASTA (Pearson 2004) with the default settings which resulted in the recognition of a number of homologous sequences from different species. The text file containing PKC $\delta$  and all its sequence homologues was then used as an input for multiple sequence alignment utilizing CLUSTALX software (Thompson, Gibson *et al.* 1997).

## RESULTS

### Sequence analysis and homology modeling of human CDDR protein

Structural homologue of human CDDR sequence was first typically searched against PDB. However, the targeted sequence did not match significantly with any of the protein in PDB. In order to construct 3D model of a protein, it is important to recognize the correct fold so that its functional analyses can be performed (Lobley, Sadowski *et al.* 2009). It is not always essential to have a significant evolutionary relationship with proteins in PDB (Bernstein, Koetzle *et al.* 1977) that can be used for correct tertiary structure prediction. However there are certain methods available which do not consider homology between the target sequence and the fragment source rather for new-fold prediction they are based on the re-use of arbitrary structural fragments (Jones 2001, Rohl, Strauss *et al.* 2004, Zhang 2007). Currently pGenTHREADER is a widely implemented method for fold recognition and discrimination of protein superfamilies (Lobley, Sadowski *et al.* 2009). Fold recognition deals with the identification of three dimensional template that possibly resembles the tertiary structure of query sequence (Al-Lazikani, Jung *et al.* 2001). Therefore during the present study, the structural homologue of human CDDR protein was identified through the process of fold recognition via pGenTHREADER method. A region (263-312) of L-aspartate- $\beta$ -decarboxylase (pdb id; 2ZY2, chain A) was found to have similar structural fold with human CDDR protein and therefore was focused as a template for homology modeling studies. The secondary structure of human CDDR protein predicted by Psi-Pred method (Jones 1999) showed three  $\beta$  strands without any regular helical segment (fig. 1A). This predicted secondary structure of human CDDR protein was in

agreement with the secondary structure of *Pseudomonas sp.* L-aspartate- $\beta$ -decarboxylase (pdb id; 2ZY2, chain A) except for one short helix present in template and found to be deleted from the target CDDR protein sequence.

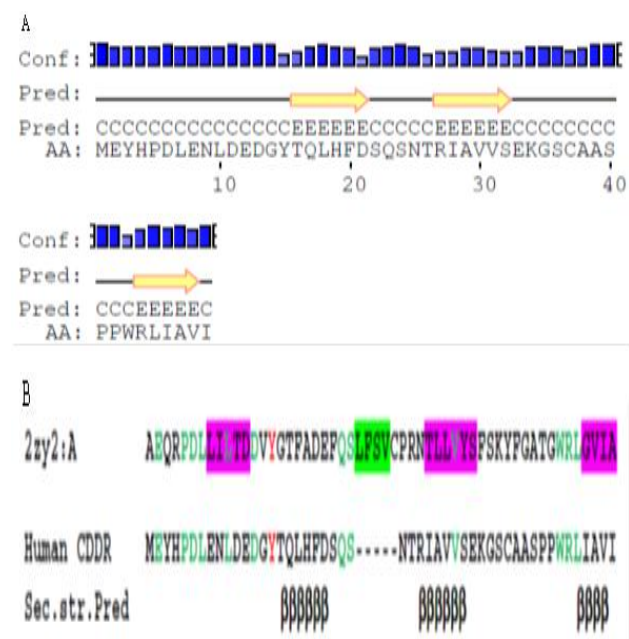


**Fig. 1:** Secondary structure prediction of human cytoplasmic domain of Dectin-1 receptor protein using Psi-Pred secondary structure prediction method [20], where C represents amino acids forming coils and E represents amino acids forming  $\beta$ -strands (A). Structure-based pairwise sequence alignment of human CDDR protein and *Pseudomonas sp.* L-aspartate  $\beta$ -decarboxylase. The  $\alpha$ -helix and  $\beta$ -strands of *Pseudomonas sp.* L-aspartate  $\beta$ -decarboxylase are highlighted in green and pink color, respectively. The symbol " $\beta$ " represents amino acid predicted to form  $\beta$ -strand of human CDDR. Conserved residues are shown in green color (B).

Structure-based pair-wise sequence alignment of human CDDR protein and *Pseudomonas sp.* L-aspartate  $\beta$ -decarboxylase was constructed considering the secondary structures of both proteins (fig.1B). The edited sequence alignment was utilized for homology model building using MODELLER 9.10 (Sali 1995) and a total of ten models were generated.

### Assessment of human CDDR protein homology model

The aforementioned models were ranked after calculating their discrete optimized potential energy (DOPE) as shown in table-1. Consequently, model number-5 was found to have the highest DOPE score (-2424.781006 KJ/mol) and thus was selected as the best model. The overall fold of the homology model was similar to that of the template which appeared to consist of three  $\beta$ -strands stacked together as a mixed  $\beta$ -sheet (fig. 2). Evaluation of homology model was carried out using various bioinformatics tools. Model stereochemistry was

investigated using Procheck (Laskowski, MacArthur *et al.* 1993) which depicted 91% and 9% amino acid residues in most favored and additionally allowed regions of Ramachandran plot, respectively. There was no residue in generously allowed and disallowed region of Ramachandran plot (fig. 3A). The overall energy profiles of both the CDDR target and template structures were obtained using PROSA (Sippl 1993). The energy profile of CDDR protein model exhibited comparatively lesser energy than that of L-aspartate  $\beta$ -decarboxylase crystal structure (fig. 3B). The total energy deviation (Z-score) of the CDDR model was determined using Prosa-Webserver (Wiederstein and Sippl 2007) and was found to be -1.11 (fig. 3C) which is quite comparable with the Z-score value (-1.21) of the L-aspartate- $\beta$ -decarboxylase (fig. 3D). The overall analysis illustrated that the constructed CDDR protein model was reliable and very close to the X-ray crystal structure of L-aspartate- $\beta$ -decarboxylase.

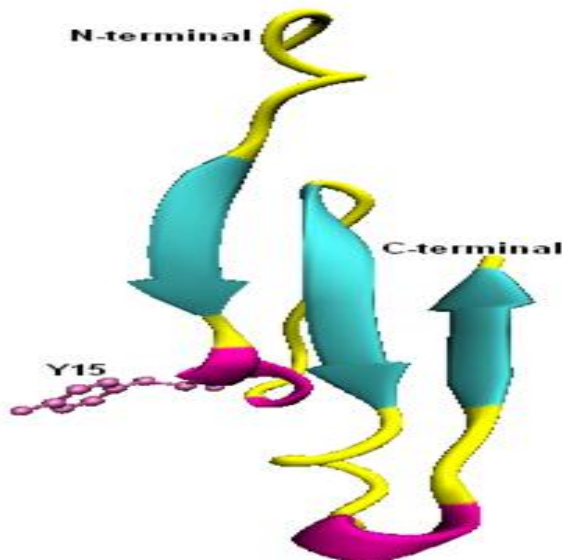


**Fig. 2:** Homology model of human cytoplasmic domain of Dectin-1 receptor (human CDDR) protein. The model shown in solid ribbon representation clearly illustrates the arrangement of three  $\beta$ -stands (cyan color) to form mixed  $\beta$ -sheet. The tyrosine residue (Y15) where phosphorylation takes place during signaling is shown in ball-and-stick representation.

#### **Molecular docking between human CDDR protein and Protein kinase C $\delta$**

In the current investigation, homology modeling depicted the location of ITAM between first two  $\beta$ -strands of CDDR protein. The key tyrosine residue (Y15) of ITAM motif which needs to be phosphorylated for signaling is shown in ball-and-stick representation (fig. 4). Previously it has been reported that PKC $\delta$  interacts with the intracellular domain of Dectin-1 receptor and this molecular complex formation is induced by zymosan. Furthermore, a direct binding between synthetic peptide (identical to the ITAM-like motif of Dectin-1 receptor) and PKC $\delta$  has been identified (Elsori, Yakubenko *et al.*

2011). To date, no work has been carried out to look into the actual pattern of molecular interaction between the two proteins. Here, we for the first time delineate the binding mode of PKC $\delta$  with CDDR protein through molecular docking studies.

We performed protein-protein docking using HADDOCK web-server, where CDDR active site was defined to be comprised of Glu12, Tyr15, Glu33, Ser36, Pro41, Arg44, Leu45 and Ile46 residues while passive residues were defined automatically by the server. As far as PKC $\delta$  active site is concerned, the complexed crystal structure of PKC $\delta$  with phosphotyrosine containing target peptide (PDB id; 1YRK) (Sondermann and Kuriyan 2005) was used to obtain the active site information by selecting amino acid residues within 5Å of the targeted peptide (the ligand). Hence, the active site of PKC $\delta$  was observed to consist of Phe4, Arg6, Lys48, Pro49, Thr50, Met51, Tyr52, Asp60, Ala61, His62, Arg67, Phe121, Leu122 and Glu123 amino acid residues. All other parameters were defined by default.

Docking using HADDOCK web-server provided us with 10 different clusters each with four different poses (table 2). We evaluated docking results by inspecting different properties of each cluster including HADDOCK score, Vander Waals energy, Electrostatic energy, Desolvation energy and Z-score. Cluster-1 showed highest HADDOCK score (-94.6  $\pm$  6.1) and best Z-score (-1.8) among all the docking clusters and represented Vander Waals and electrostatic energy to be -50.2  $\pm$  1.9 and -134.0  $\pm$  18.9, respectively, which showed the protein-protein interface to be comparatively more hydrophobic with few electrostatic interactions. Molecular interaction analysis using Dimplot suggested six hydrogen bonds between four amino acid residues of PKC $\delta$  and five residues of CDDR protein. The key residue of CDDR binding site i.e. Tyr-15, has been predicted to form ionic interaction with Glu123 of PKC $\delta$  protein. Furthermore, Leu18, Ser36, Cys37 and Trp43 of CDDR protein were found to make hydrogen bonds with Arg67, Lys48, Lys48 and Glu54 of PKC $\delta$  protein, respectively (fig. 4).

Seven amino acid residues of CDDR including Pro12, Gln17, His19, Phe20, Ala38, Ala39, Pro41 were predicted to form Vander Waals interactions with eleven amino acid residues i.e. Phe4, Gln34, Val45, Lys47, Met51, Pro53, Thr58, Phe59, Asp60, His62 and Tyr64 of PKC $\delta$  protein (fig.4).

Six amino acids of PKC $\delta$  protein were observed to surround Tyr15 residue of CDDR which were identified as Met1, Ala2, Phe4, Arg6, His62 and Glu123 residues (fig. 5A). The conservation of these six residues were evaluated within PKC $\delta$  protein sequences from seven different species using multiple sequence alignment (fig. 5B) which indicates their strict conservation across different species.

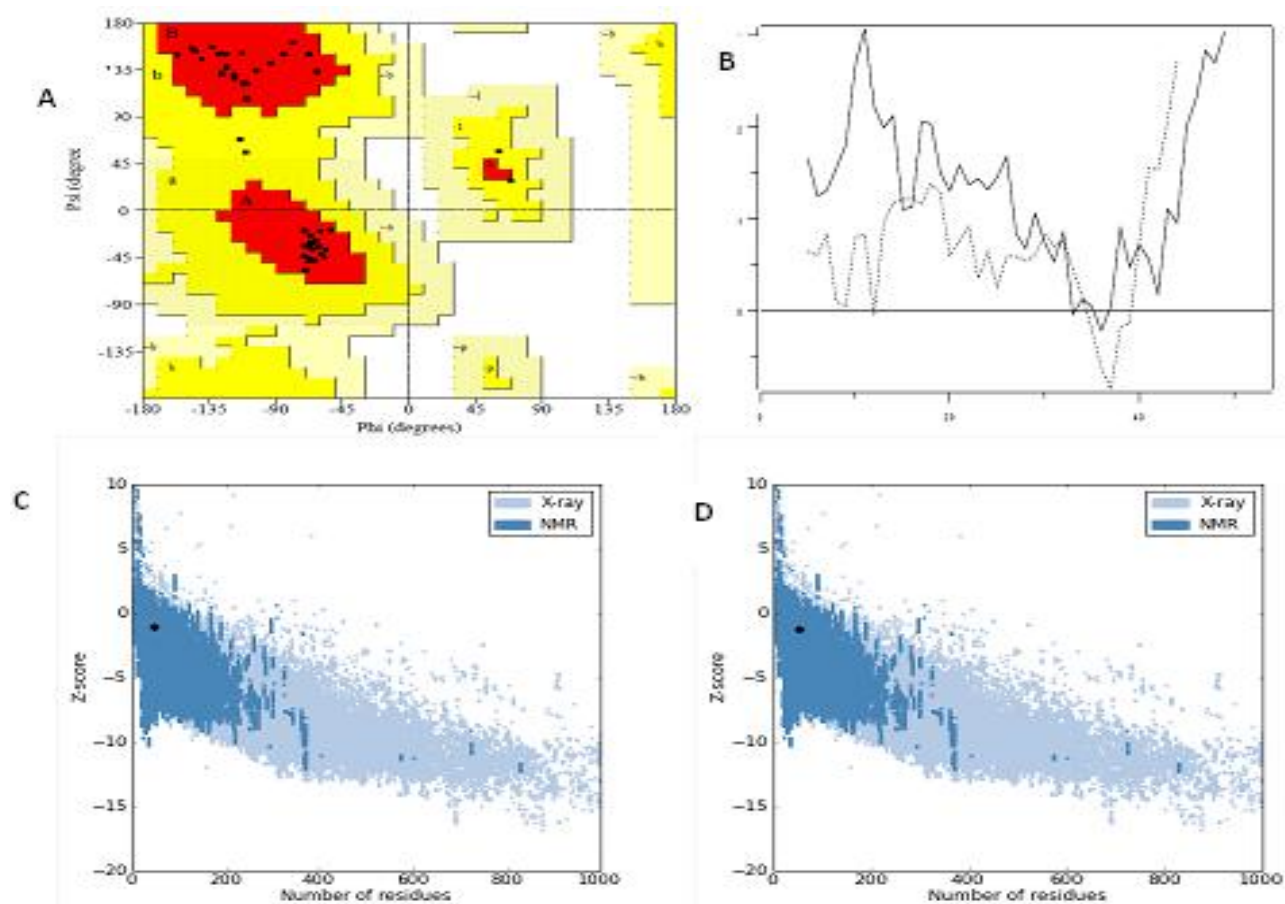


**Fig. 3:** Evaluation of human CDDR model. Stereochemical analysis was carried out using Ramachandran plot (A), energy profile of the model and template was obtained using PROSA where, the energy plot for human CDDR homology model is shown as dashedline and *Pseudomonas sp.* L-aspartate  $\beta$ -decarboxylase crystal structure (template) as solid line (B). Z-score of model (C) and template (D) was calculated using Prosa-Web and was found to be -1.11 and -1.21, respectively.

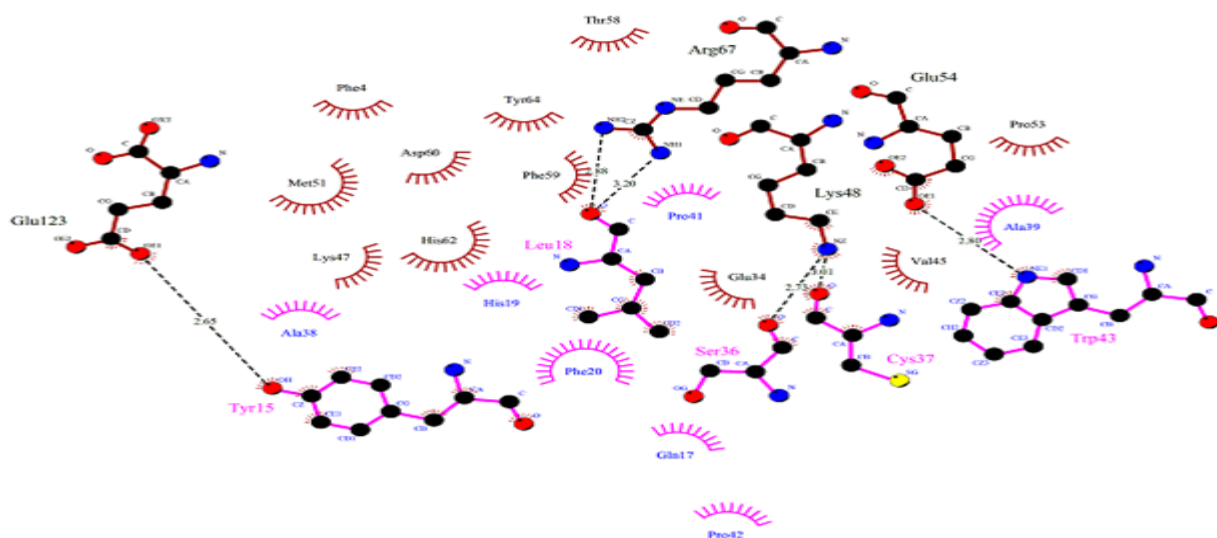
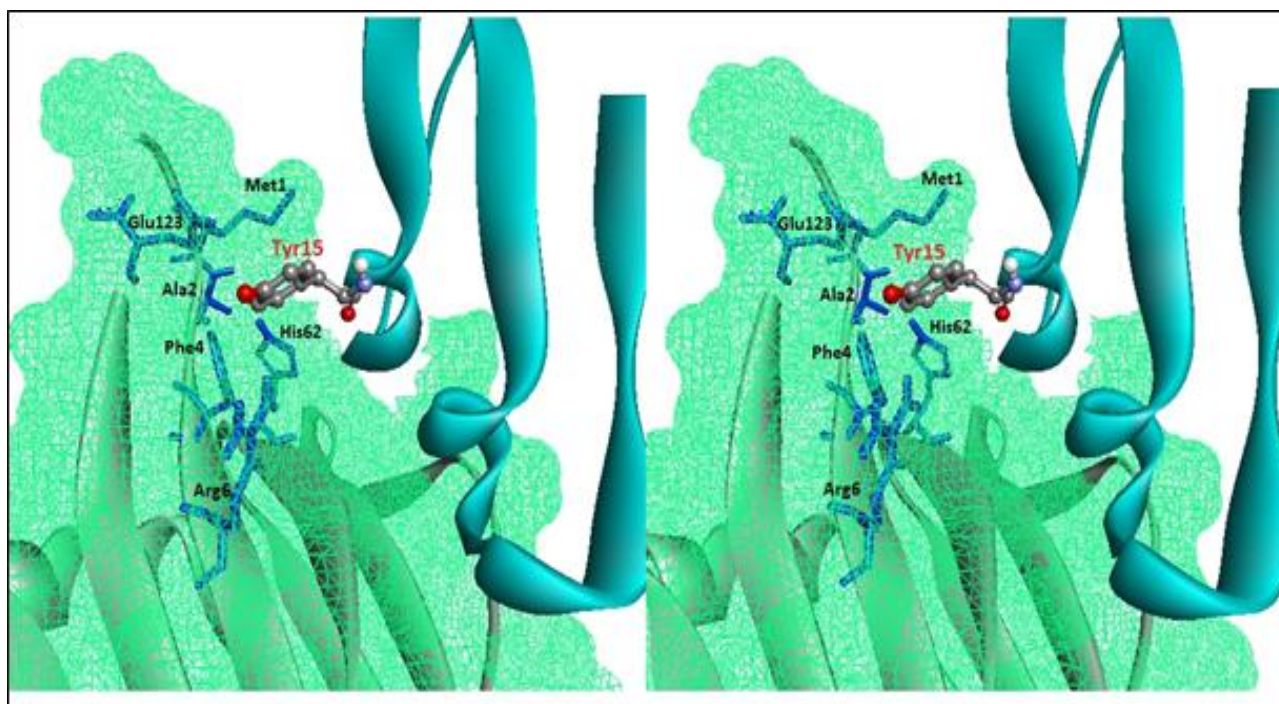


**Fig. 4:** CDDR (Ligand; pink) and PKC $\delta$  (Receptor; brown) protein-protein interaction analysis using Dimplot command of LigPlus software [31]. Hydrogen bonds between PKC $\delta$  and CDDR proteins are shown as dashed line where bond length is also mentioned.

A



B

Q7SZH8	<b>MS</b> PFLRISFN <span style="color:red">S</span> FDLGGMLSPSDHNQPFCAVKVKESL <span style="color:red">T</span> TERGKTLVQKKPTMYPDWKSVFD
Q6DCJ8	<b>MS</b> PFLRISFN <span style="color:red">S</span> FDLGGMISPSDHNQPFCAVKVKESL <span style="color:red">T</span> TERGKTLVQKKPTMYPDWKSVFD
Q7SZH7	<b>MA</b> PFLRLSFNSFDLGGMLSPSEHIQPFCAVKVKESL <span style="color:red">T</span> TERGKTLVQKKPTMYPDWKSPFD
Q498G7	<b>MA</b> PFLRLSFNSFDLGGMLSPSEHIQPFCAVKVKESL <span style="color:red">T</span> TERGKTLVQKKPTMYPDWKSPFD
P09215	<b>MA</b> PFLRISFN <span style="color:red">S</span> YELGSLQAEDDASQPFCAVKMKEAL <span style="color:red">T</span> DRGKTLVQKKPTMYPEWKSTFD
P28867	<b>MA</b> PFLRISFN <span style="color:red">S</span> YELGSLQVEDEASQPFCAVKMKEAL <span style="color:red">S</span> TERGKTLVQKKPTMYPEWKTFD
Q05655	<b>MA</b> PFLRIAFN <span style="color:red">S</span> YELGSLQAEDANQPFCAVKMKEAL <span style="color:red">S</span> TERGKTLVQKKPTMYPEWKSTFD
	*:****::**::**::: .: *****;*:*;*:*****;::: **
Q7SZH8	AH <span style="color:red">I</span> YEGRVIQIVLMKAAEDPLSEATVGVSVLAERCKKGNKSEFWLDLQPQAKVLM <span style="color:red">S</span> VQY
Q6DCJ8	AH <span style="color:red">I</span> YEGRVIQIVLMKAAEDPLSEATVGVSVLAERCKKGNKSEFWLDLQPQAKVLM <span style="color:red">S</span> VQY
Q7SZH7	AH <span style="color:red">I</span> YEGRVIQIVLMKA <span style="color:red">V</span> EDPLSEATVGVSVLAERCKKGNKSEFWLDLQPQAKVLM <span style="color:red">S</span> VQY
Q498G7	AH <span style="color:red">I</span> YEGRVIQIVLMKAAEDPLSEATVGVSVLAERCKKGNKSEFWLDLQPQAKVLM <span style="color:red">S</span> VQY
P09215	AH <span style="color:red">I</span> YEGRVIQIVLMRAAEDPMSEVTVGVSVLAERCKKNGKA <span style="color:red">E</span> FWLDLQPQAKVLM <span style="color:red">C</span> VQY
P28867	AH <span style="color:red">I</span> YEGRVIQIVLMRAAEDPVSEVTVGVSVLAERCKKNGKA <span style="color:red">E</span> FWLDLQPQAKVLM <span style="color:red">C</span> VQY
Q05655	AH <span style="color:red">I</span> YEGRVIQIVLMRAAEEPVSEVTVGVSVLAERCKKNGKA <span style="color:red">E</span> FWLDLQPQAKVLM <span style="color:red">S</span> VQY
	*****:*. *:*:*..*****.***;*****.***
Q7SZH8	FL <span style="color:red">E</span> DADLKQSIR-EDEGLVTINKRRGAIKQAKIHYIKNHEFTATFFGQPTFCSVCRE <span style="color:red">F</span> VW
Q6DCJ8	FL <span style="color:red">E</span> DADLKQSIR-EDEGLVTINKRRGAIKQAKIHYIKNHEFTATFFGQPTFCSVCRE <span style="color:red">F</span> VW
Q7SZH7	FL <span style="color:red">E</span> DADLKQSIR-EDEGLVTINRRRGAIKQAKIHYIKNHEFIATFFGQPTFCSVCRE <span style="color:red">F</span> VW
Q498G7	FL <span style="color:red">E</span> DADLKQSIR-EDEGLVTINRRRGAIKQAKIHYIKNHEFIATFFGQPTFCSVCRE <span style="color:red">F</span> VW
P09215	FL <span style="color:red">E</span> DGDCKQSMRSEEEAMFPTMNRGAIKQAKIHYIKNHEFIATFFGQPTFCSVCKE <span style="color:red">F</span> VW
P28867	FL <span style="color:red">E</span> DGDCKQSMRSEEEAKFPTMNRGAIKQAKIHYIKNHEFIATFFGQPTFCSVCKE <span style="color:red">F</span> VW
Q05655	FL <span style="color:red">E</span> DVDCKQSMRSEDEAKFPTMNRGAIKQAKIHYIKNHEFIATFFGQPTFCSVCK <span style="color:red">D</span> FW
	**** * **:* *:*..*****.*****;*****;***

**Fig. 5:** Analysis of Tyr15 (included in ITAM of CDDR protein) interaction with PKC $\delta$  protein and its conservation across different species: Tyr15 of CRRD protein is represented as ball-and-stick representation while amino acid residues of PKC $\delta$  protein around 5A° of Tyr15 are depicted in blue stick representation (A); N-terminal portion of multiple sequence alignment of seven PKC $\delta$  protein sequences is depicted (B) where amino acid residues of Tyr15-binding pocket are shown in red color.

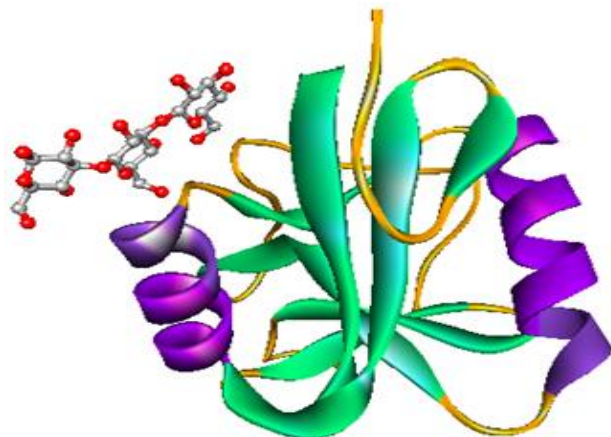


**Fig. 6:** Homology model of CTLD of human Dectin-1 receptor complexed with  $\beta$ -glucan. Helices and  $\beta$ -sheets are shown in purple and green color, respectively.  $\beta$ -glucan is shown in ball-and-stick representation.

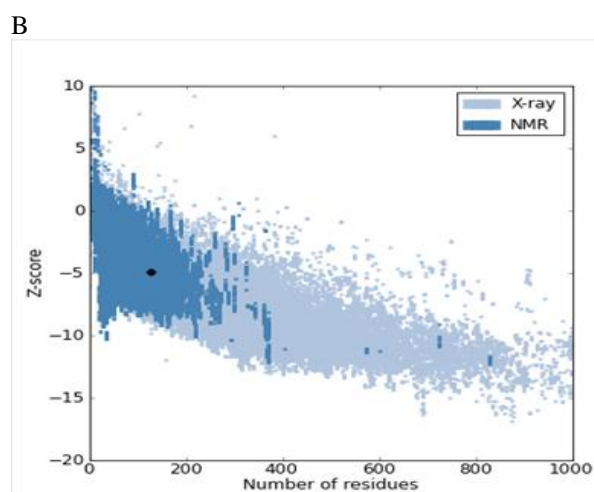
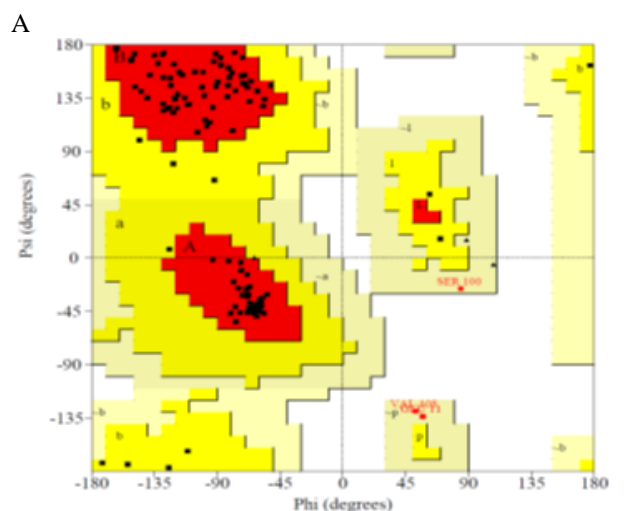


**Fig. 7:** Evaluation of human CTLD model stereochemical analysis was carried out using Ramachandran plot (A) while z-score of CTLD model was determined by Prosa-Web server and was found to be -4.89 (B).

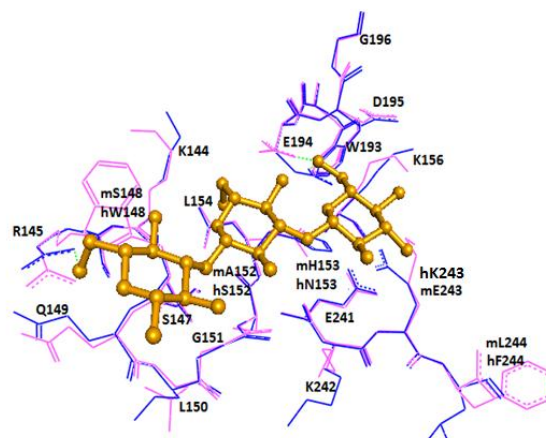


**Fig. 8:** Comparison of murine CTLD (blue/m) and human CTLD (pink/h)  $\beta$ -glucan binding pocket. All the residues are labeled.  $\beta$ -glucan is shown in yellow colored ball-and-stick representation.

#### Sequence retrieval and homology modeling of human CTLD

Human CTLD protein sequence in FASTA format was obtained from UniProtKb (Magrane and Consortium 2011) and was searched against PDB (Bernstein, Koetzle *et al.* 1977) using Psi-BLAST tool (Altschul, Madden *et al.* 1997). Murine Dectin-1 CTLD complexed with  $\beta$ -glucan was found to be the best hit having 60% sequence identity. The obtained alignment was used to make five initial models which were assessed for their compatibility. Model-3 was found to be the best model (fig. 6) on the basis of stereochemistry (fig. 7A) and Z-score analysis (fig. 7B). There is no any residue in the disallowed region, 3 residues in the generously allowed, 11 residues in the additional allowed and 98 residues in the most favored region of the Ramachandran plot. Z-score of model and template was found to be -4.89 and -5.57, respectively, suggesting compatibility between the two structures. The amino acid residues within CTLD  $\beta$ -glucan binding pockets of both human and murine Dectin-1 were compared after superposition (fig. 8). Seventeen amino acid residues falling within  $8\text{\AA}$  of the  $\beta$ -glucan molecule were considered as potential constituents of the binding pocket. Out of seventeen, twelve amino acid residues were conserved in human CTLD. Two hydrogen bonds between CTLD and  $\beta$ -glucan were observed in both human and murine structures involving the conserved E194 and R145 residues. Five substitutions from murine to human were identified including A152 $\rightarrow$ S152, H153 $\rightarrow$ N153 and E243 $\rightarrow$ K243 to be conservative while L244 $\rightarrow$ F244 and S148 $\rightarrow$ W148 to be non-conservative changes.

#### DISCUSSION

Stimulation of Dectin-1 receptor with  $\beta$ -glucan and its downstream signaling involves direct interaction between protein kinase C $\delta$  and ITAM motif of CDDR to regulate

**Table 1:** Comparative study of DOPE scores of ten homology models predicted through MODELLER v9.10

S.No.	Model predicted through modeller	DOPE (KJ/mol)
1	HUMAN CDDR.B99990001	-2419.738525
2	HUMAN CDDR.B99990002	-2279.046631
3	HUMAN CDDR.B99990003	-2384.759521
4	HUMAN CDDR.B99990004	-2308.927002
5	HUMAN CDDR.B99990005	-2424.781006
6	HUMAN CDDR.B99990006	-2302.704590
7	HUMAN CDDR.B99990007	-2252.474121
8	HUMAN CDDR.B99990008	-2134.518555
9	HUMAN CDDR.B99990009	-2116.400146
10	HUMAN CDDR.B999900010	-2308.892822

**Table 2:** HADDOCK docking results of CDDR (Ligand) and Protein kinase-C delta (Receptor)

Cluster No.	HADDOCK score	Van Der Waal's energy	Electrostatic energy	Desolvation energy	Z-score
1	-94.6 +/- 6.1	-50.2 +/- 1.9	-134.0 +/- 18.9	-21.0 +/- 0.9	-1.8
2	-87.0 +/- 2.1	-45.1 +/- 7.0	-115.5 +/- 15.4	-20.2 +/- 5.3	-1.1
3	-84.2 +/- 3.5	-33.4 +/- 2.3	-179.5 +/- 18.6	-18.9 +/- 7.4	-0.8
4	-72.8 +/- 3.1	-37.8 +/- 12.1	-215.1 +/- 95.3	-0.8 +/- 7.7	0.3
5	-69.1 +/- 6.5	-34.6 +/- 8.8	-136.4 +/- 17.3	-11.3 +/- 6.3	0.6
6	-83.7 +/- 10.3	-47.0 +/- 8.0	-81.9 +/- 28.5	-23.7 +/- 6.2	-0.8
7	-72.6 +/- 11.1	-11.9 +/- 4.3	-362.8 +/- 42.5	6.3 +/- 15.4	0.3
8	-64.4 +/- 3.3	-31.7 +/- 6.4	-103.0 +/- 8.6	-13.3 +/- 4.7	1.1
9	-59.9 +/- 0.9	-34.8 +/- 1.4	-57.2 +/- 22.7	-16.1 +/- 5.8	1.5
10	-69.9 +/- 16.7	-27.6 +/- 10.4	-198.1 +/- 38.4	-5.4 +/- 5.3	0.6

NADPH oxidase-dependent superoxide anion generation, cytokines production and phagocytosis of fungal pathogens (Elsori, Yakubenko *et al.* 2011). Being an integral membrane protein, Dectin-1 receptor has three well-defined domains including extracellular CTLD at the C-terminus, a transmembrane region and a cytoplasmic tail with ITAM motif at N-terminus (Ariizumi, Shen *et al.* 2000). The 3D structure of Dectin-1 from Murine and *Bubalus bubalis* and its interaction with  $\beta$ -glucan has been previously described (Brown, O'Callaghan *et al.* 2007, Yadav, Tripathi *et al.* 2012). However, structural elucidation of human Dectin-1 receptor and its detailed interaction with  $\beta$ -glucan and with intracellular signaling components in regulating fungus-mediated immune response has not been investigated so far. Considering the importance of human CTLD and CDDR in recognizing pathogen-derived  $\beta$ -glucan and mediating downstream signaling, we performed their structural characterization and molecular interaction analysis with  $\beta$ -glucan and PKC $\delta$ , respectively, in order to understand the fundamentals of protective immune response against fungal pathogens.

Human CDDR homology modeling reveals the overall tertiary structure consisting of three  $\beta$ -strands arranged as a mixed  $\beta$ -sheet containing only one Y15-ITAM with YXXL motif. A typical ITAM motif has two tyrosine residues arranged as dual YXXL motif and

phosphorylation of both tyrosine residues are required for downstream signaling. However, in case of the lectin receptors i.e. Dectin-1 and CLEC-2, there is only a single YXXL motif in the cytoplasmic tail and tyrosine phosphorylation of this motif is thought to be sufficient to initiate downstream signaling (Rogers, Slack *et al.* 2005, Fuller, Williams *et al.* 2007). Previous study showed that stimulation of Dectin-1 with  $\beta$ -glucan, the intracellular phosphorylated PKC $\delta$  forms a complex with phosphotyrosine-containing ITAM of CDDR to regulate different immune/inflammatory pathways in human monocytes (Elsori, Yakubenko *et al.* 2011). Therefore in order to have an idea about the conformation and chemistry of PKC $\delta$  and CDDR protein-protein interface, we performed molecular docking studies. There are comparatively more hydrophobic residues exist at the interface which are found to be involved in Vander Waals interactions that reciprocate with the calculated Vander Waals energy. The tyrosine15 (Y15) binding pocket of PKC $\delta$  suggests a shallow groove having partial hydrophobic and hydrophilic residues which are conserved across different species showing their significant role in binding with Y15 of CDDR. Interestingly, both the N- and C-terminal residues of PKC $\delta$  were found to involve in interacting with Y15. The interaction analysis of CDDR and PKC $\delta$  will be a milestone in drug discovery programs for introducing various protein inhibitors that can either interfere with

various inflammatory responses, intracellular production of NADPH oxidase-dependent superoxide anion and phagocytosis during fungal and/or bacterial infections. Additionally, CDDR structure-based drugs will provide new insights into the intervention of atherosclerosis and chronic granulomatous disease.

Targeting CTLD indeed is another aspect of drug discovery to deal with the deleterious fungal infections as well as immunization. We provided a 3D model of human CTLD complexed with  $\beta$ -glucan, the overall architecture of human CTLD comprises of one long loop region (LLR; consisting of 35 residues) and two three-stranded antiparallel  $\beta$ -sheets flanked by two  $\alpha$ -helices. The  $\beta$ -glucan binding pocket of human CTLD was found to be 70% identical to that of murine CTLD (Brown, O'Callaghan *et al.* 2007). Three of the substituted residues of human CTLD (murine $\rightarrow$ human; A152 $\rightarrow$ S152, H153 $\rightarrow$ N153, K243 $\rightarrow$ E243) showed similar chemical properties in comparison with those of murine CTLD. The mutation (S148 $\rightarrow$ W148) was observed 8Å apart from the ligand which due to its distal location does not seem to have any significant influence on the binding-site chemistry. Whereas, the aliphatic to aromatic evolutionary change (murine $\rightarrow$ human; L244 $\rightarrow$ F244) could exert only a minor impact on the ligand binding phenomenon because of the same hydrophobic nature of these amino acids. Regarding the chemistry of human  $\beta$ -glucan binding-site, we postulate that the ligand interacts with human CTLD almost in a similar fashion as it does with murine CTLD (Rogers, Slack *et al.* 2005).

Fungi have been recognized as a crucial human pathogen that are involved in various diseases which contribute substantially to worldwide morbidity and mortality (Brown, Denning *et al.* 2012). The diversity in fungal pathogens and related drug resistance demands to understand immune response against fungi. Currently, the role of CTLDs especially Dectin-1 in recognition of pathogens in innate immune system is of great significance.

## CONCLUSION

The present work provides the 3D structural models of human CDDR and CTLD of Dectin-1 and their molecular interaction pattern with PKC $\delta$  (a critical downstream signaling component of Dectin-1) and  $\beta$ -glucan (a fungal pathogen stimulator of Dectin-1), respectively, that can be implicated in the structure-based drug designing for immunomodulatory therapy to control fungal infections and/or to potentiate the host defense as well as to treat chronic immuno-inflammatory diseases.

## REFERENCES

Adachi Y, T Ishii, Y Ikeda, A Hoshino, H Tamura, J Aketagawa, S Tanaka and N Ohno (2004).

- Characterization of beta-glucan recognition site on C-type lectin, dectin 1. *Infect Immun.*, **72**(7): 4159-4171.
- Al-Lazikani B, J Jung, Z Xiang and B Honig (2001). Protein structure prediction. *Curr. Opin. Chem. Biol.*, **5**(1): 51-56.
- Altschul SF, TL Madden, AA Schaffer, J Zhang, Z Zhang, W Miller and DJ Lipman (1997). Gapped BLAST and PSI-BLAST: A new generation of protein database search programs. *Nucleic Acids Res.*, **25**(17): 3389-3402.
- Ariizumi K, GL Shen, S Shikano, S Xu, R Ritter, 3rd, T Kumamoto, D Edelbaum, A Morita, PR Bergstresser and A Takashima (2000). Identification of a novel, dendritic cell-associated molecule, dectin-1, by subtractive cDNA cloning. *J. Biol. Chem.*, **275**(26): 20157-20167.
- Azim YRAMK (2011). Comparative modeling of Anhydro-N-Acetylmuramyl-L-Ala Amidase from *Neisseria meningitidis*: Implications for structure-function relationship. *Pak. J. Biochem. Mol. Biol.*, **44**(4): 153-155.
- Bernstein FC, TF Koetzle, GJ Williams, EF Meyer, Jr, MD Brice, JR Rodgers, O Kennard, T Shimanouchi and M Tasumi (1977). The Protein Data Bank: a computer-based archival file for macromolecular structures. *J. Mol. Biol.*, **112**(3): 535-542.
- Brown GD, DW Denning, NA Gow, SM Levitz, MG Netea and TC White (2012). Hidden killers: human fungal infections. *Sci. Transl. Med.*, **4**(165): 165rv13.
- Brown GD and S Gordon (2001). Immune recognition. A new receptor for beta-glucans. *Nature*, **413**(6851): 36-37.
- Brown GD, J Herre, DL Williams, JA Willment, AS Marshall and S Gordon (2003). Dectin-1 mediates the biological effects of beta-glucans. *J. Exp. Med.*, **197**(9): 1119-1124.
- Brown J, CA O'Callaghan, AS Marshall, RJ Gilbert, C Siebold, S Gordon, GD Brown and EY Jones (2007). Structure of the fungal beta-glucan-binding immune receptor dectin-1: implications for function. *Protein Sci.*, **16**(6): 1042-1052.
- Cathcart MK (2004). Regulation of superoxide anion production by NADPH oxidase in monocytes/macrophages: Contributions to atherosclerosis. *Arterioscler Thromb. Vasc. Biol.*, **24**(1): 23-28.
- Cathcart MK, AK McNally, DW Morel and GM Chisolm, 3rd (1989). Superoxide anion participation in human monocyte-mediated oxidation of low-density lipoprotein and conversion of low-density lipoprotein to a cytotoxin. *J. Immunol.*, **142**(6): 1963-1969.
- de Vries SJ and AM Bonvin (2011). CPORT: a consensus interface predictor and its performance in prediction-driven docking with HADDOCK. *PLoS One*, **6**(3): e17695.
- de Vries SJ, M van Dijk and AMJJ Bonvin (2010). The HADDOCK web server for data-driven biomolecular docking. *Nat. Protocols.*, **5**(5): 883-897.

- Elsori DH, VP Yakubenko, T Roome, PS Thiagarajan, A Bhattacharjee, SP Yadav and MK Cathcart (2011). Protein kinase Cdelta is a critical component of Dectin-1 signaling in primary human monocytes. *J. Leukoc. Biol.*, **90**(3): 599-611.
- Fuller GL, JA Williams, MG Tomlinson, JA Eble, SL Hanna, S Pohlmann, K Suzuki-Inoue, Y Ozaki, SP Watson and AC Pearce (2007). The C-type lectin receptors CLEC-2 and Dectin-1, but not DC-SIGN, signal via a novel YXXL-dependent signaling cascade. *J. Biol. Chem.*, **282**(17): 12397-12409.
- Gantner BN, RM Simmons, SJ Canavera, S Akira and DM Underhill (2003). Collaborative induction of inflammatory responses by dectin-1 and Toll-like receptor 2. *J. Exp. Med.*, **197**(9): 1107-1117.
- Jones DT (1999). Protein secondary structure prediction based on position-specific scoring matrices. *J. Mol. Biol.*, **292**(2): 195-202.
- Jones DT (2001). Predicting novel protein folds by using FRAGFOLD. *Proteins Suppl.*, **5**: 127-132.
- Laskowski RA, MW MacArthur, DS Moss and JM Thornton (1993). PROCHECK: A program to check the stereochemical quality of protein structures. *J. Appl. Cryst.*, **26**(2): 283-291.
- Laskowski RA and MB Swindells (2011). LigPlot+: multiple ligand-protein interaction diagrams for drug discovery. *J. Chem. Inf. Model*, **51**(10): 2778-2786.
- Lobley A, MI Sadowski and DT Jones (2009). pGenTHREADER and pDomTHREADER: New methods for improved protein fold recognition and superfamily discrimination. *Bioinformatics.*, **25**(14): 1761-1767.
- Magrane M, and U Consortium (2011). UniProt Knowledgebase: A hub of integrated protein data. Database (Oxford) 2011: bar009.
- McGuffin LJ, K Bryson and DT Jones (2000). The PSIPRED protein structure prediction server. *Bioinformatics*, **16**(4): 404-405.
- Pearson W (2004). Finding protein and nucleotide similarities with FASTA. *Curr. Protoc. Bioinformatics*, Chapter 3: Unit3 9.
- Rashid Y and M Kamran Azim (2011). Structural bioinformatics of *Neisseria meningitidis* LD-carboxypeptidase: Implications for substrate binding and specificity. *Protein J.*, **30**(8): 558-565.
- Rashid Y, M Kamran Azim, ZS Saify, KM Khan and R Khan (2012). Small molecule activators of proteasome-related HsIV peptidase. *Bioorg Med. Chem. Lett.*, **22**(19): 6089-6094.
- Rogers NC, EC Slack, AD Edwards, MA Nolte, O Schulz, E Schweighoffer, DL Williams, S Gordon, VL Tybulewicz, GD Brown and C Reis e Sousa (2005). Syk-dependent cytokine induction by Dectin-1 reveals a novel pattern recognition pathway for C type lectins. *Immunity*, **22**(4): 507-517.
- Rohl CA, CE Strauss, KM Misura and D Baker (2004). Protein structure prediction using Rosetta. *Methods Enzymol.*, **383**: 66-93.
- Sali A (1995). Modeler: Implementing 3D protein modeling. MC2 Molecular Simulations Inc., Burlington, MA.
- Salvemini D, E Mazzon, L Dugo, DP Riley, I Serraino, AP Caputi and S Cuzzocrea (2001). Pharmacological manipulation of the inflammatory cascade by the superoxide dismutase mimetic, M40403. *Br. J. Pharmacol.*, **132**(4): 815-827.
- Sippl MJ (1993). Recognition of errors in three-dimensional structures of proteins. *Proteins*, **17**(4): 355-362.
- Sondermann H and J Kuriyan (2005). C2 Can Do It, Too. *Cell*, **121**(2): 158-160.
- Taylor PR, GD Brown, DM Reid, JA Willment, L Martinez-Pomares, S Gordon and SY Wong (2002). "The beta-glucan receptor, dectin-1, is predominantly expressed on the surface of cells of the monocyte/macrophage and neutrophil lineages. *J. Immunol.*, **169**(7): 3876-3882.
- Thompson JD, TJ Gibson, F Plewniak, F Jeanmougin and DG Higgins (1997). The CLUSTAL\_X windows interface: flexible strategies for multiple sequence alignment aided by quality analysis tools. *Nucleic Acids Res.* **25**(24): 4876-4882.
- Underhill DM (2007). Collaboration between the innate immune receptors dectin-1, TLRs and Nods. *Immunol. Rev.* **219**: 75-87.
- Underhill DM, E Rossnagle, CA Lowell and RM Simmons (2005). Dectin-1 activates Syk tyrosine kinase in a dynamic subset of macrophages for reactive oxygen production. *Blood*, **106**(7): 2543-2550.
- Wiederstein M and MJ Sippl (2007). ProSA-web: interactive web service for the recognition of errors in three-dimensional structures of proteins. *Nucleic Acids Res.*, **35**(Web Server issue): W407-410.
- Yadav BS, V Tripathi, A Kumar, MF Khan, A Barate, A Kumar and B Sharma (2012). Molecular modeling and docking characterization of Dectin-1 (PAMP) receptor of *Bubalus bubalis*. *Exp. Mol. Pathol.*, **92**(1): 7-12.
- Zhang Y (2007). Template-based modeling and free modeling by I-TASSER in CASP7. *Proteins*, **69**(Suppl 8): 108-117.